IJAREEIE

e-ISSN: 2278-8875
p-ISSN: 2320-3765

International Journal of Advanced Research in Electrical, Electronics and Instrumentation Engineering

Volume 11, Issue 2, February 2022

ISSN INTERNATIONAL STANDARD SERIAL NUMBER INDIA

Impact Factor: 7.282

| e-ISSN: 2278 – 8875, p-ISSN: 2320 – 3765| www.ijareeie.com | Impact Factor: 7.282|

|| Volume 11, Issue 2, February 2022 ||

DOI:10.15662/IJAREEIE.2022.1102015

Mechano-Dynamic Model for Biosignal Processing

Chetana Krishnan[1], Hariprasad Kuruppassery[2], Aishwarya Sathe[3]

UG Student, Dept. of Biomedical Engineering, SSN College of Engineering, Tamilnadu, India[1]
Senior Systems Engineer, Infosys Limited[2]
Technical Associate, Learnbyresearch, India[3]

ABSTRACT: Instantaneous and continuous monitoring is required for remote data acquisition from patients to make treatments better during pandemic situations. The proposed solution brings up a mechanical model to study the pathways and regulatory responses of the biosignals like Cardiogram and Spirogram to determine the progress of the physiological system towards a disease. The model also compares 2 elements, 3 elements, and 4 elements, hemo models, for the best processing of biosignals. Circuit parameters like state of art, arterial flow, compliance rate, etc were calculated. With the Q factor resemblance, the cardio-pneumatic healthiness was determined.

KEYWORDS: dynamic, pneumatic signals, arterial flow, hemo-mechanics, state of art, transmission.

I. INTRODUCTION TO PHYSIOLOGICAL MODELS

The vascular and pneumatic system of the body composes the heart, the lungs, and its connecting blood vessels[1][2]. The two types of circulation – systemic that distribute oxygen-rich blood to the body, deoxygenated blood back to the heart, and pulmonary that forms the closed division to the systemic circulation. The valves play the role of connectors by interlinking the forward and the back flow of the blood. Cardiovascular diseases alter this flow rate and cause inhibitory actions which take massive pathological or blockage effects. Real-time switches in electronics are analogous to the valves in physiology. A similar response is found in the pneumatic system as well where compliance and lung elasticity play a huge role in exchanging air in and out the body[3].

A. Cardiovascular Physiology and Its Mechanics

The entire circulation starts from the right atrium flow to the left ventricular terminal. The blood stored in the right atrium is pushed to the right ventricle by the tricuspid valves[4][5]. The valve pressure is constantly maintained by the tissues surrounding it. The flow rate decreases as the blockage increase in the valve. The pulmonary artery transports the blood to the lungs and is bought back to the left ventricle. The bicuspid valve functions in the case of the left septum of the heart. Apart from bi and tricuspid valves, many interconnected valves work together to promote the flow of blood which is a bit complex to understand. The above model can be electrically represented as shown in figure 1. The resistors in parallel with the capacitors represent the veins (pulmonary and arterial). The series of resistors represent the microcirculation followed by the capacitor pairs that represent the arterial flow (pulmonary artery). The mechanism of blood flow is driven by the current where the probe at the end reads an excitation voltage of 5 volts. Any change to the resistance will lead to a change in current and voltage. The diodes act as the switching valves here which based on the bias operate the circuit in either open or closed mode. During forward bias (systemic circulation), the tricuspid valves are closed and during reverse bias (pulmonary circulation), the bicuspid valves are closed. The model is simulated using Multisim.

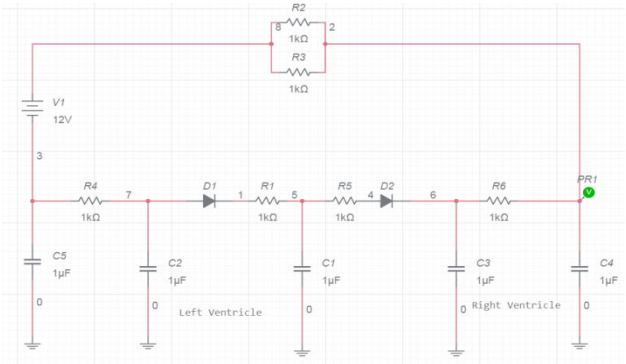

Fig.1. Cardiovascular Lumped Model

| e-ISSN: 2278 – 8875, p-ISSN: 2320 – 3765| www.ijareeie.com | Impact Factor: 7.282|

|| Volume 11, Issue 2, February 2022 ||

DOI:10.15662/IJAREEIE.2022.1102015

Figure 2 shows the output of the model where the front traced line is the reference and the backtraced line is the reference. The phase delay shows the time lag that the mechanical model achieves, unlike the physiological model. To avoid the delay, a timer with the customized flow rate can be inserted in the model.

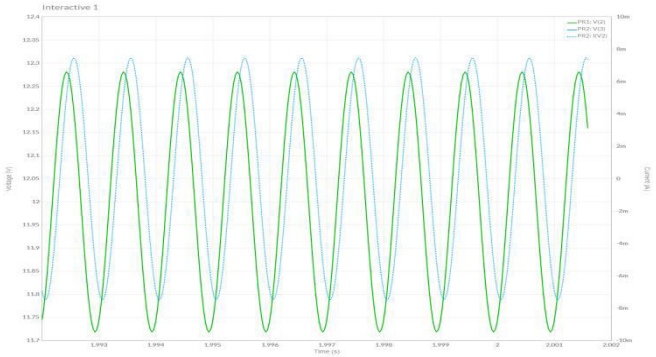

Fig.2. Cardiovascular Lumped Output

B. Pneumatic Physiology and Its Mechanics

The lung mechanics constitutes the inspiration and expiration where pressure difference plays a vital role. When the volume of the thoracic cavity increases, the pressure within the lung decreases leading to the movement of air from the outside to the lungs (inspiration). As the pressure neutralises in the lungs, the volume increases leading to the movement of air from the lungs to the outside (expiration)[6]. The capacity rate of the lungs to expand and contract is termed as compliance rate. Destruction in the normal pressure Vs volume ratio can lead to diseases like asthma or Chronic Obstructive Pulmonary Disease. Figure 3 shows the corresponding mechanical model of the lungs. The series RL branches represent the upper and lower airways with a small difference in resistance that acts like the diaphragm in the physiological model. The pair of RC circuits represent the bronchi branches from which the air (current) flows. Two probes – excitation and reference read the upper and lower responses.

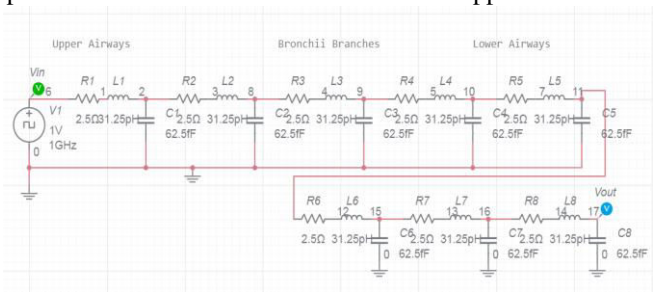

Fig.3. Pneumatic Lumped Model

The input is a pulse train with a 1ns lag duration to correspond to 11 breathes per minute in real-time. Figure 4 shows the model output. The reference voltage (green) is the ideal case where no air is trapped in the bronchi layer, only a steep is formed between upper and lower responses. In the case of practical response (blue), a transiency is seen between the upper and lower points indicating that the air takes pulse delays in reaching the alveoli. When the same model is constructed using distributed systems, this lag can be avoided by introducing parallel networks.

| e-ISSN: 2278 – 8875, p-ISSN: 2320 – 3765| www.ijareeie.com | Impact Factor: 7.282|

|| Volume 11, Issue 2, February 2022 ||

DOI:10.15662/IJAREEIE.2022.1102015

Fig.4. Pneumatic Lumped Output

C. Hemodynamics and Its Mechanics

Hemodynamics refers to the blood flow in the interior parts of the body which constitutes three main processes – hydrostatic (due to static valve resistance), isostatic (due to constant valve resistance), and hypostatic (due to decreased valve resistance)[7]. The former is due to the change in the velocity of blood as the result of pressure changes. The latter is due to the changes in the cross-sectional area of the valves. Hemodynamics plays a significant role in analyzing cardiac diseases. The change in the flow rate can be electrically represented as shown in figure 5. The RC series pair represent the hydrated flow whose time constant will be equal to the steady flow rate. The time constant is given by equation 1[8].

$$\tau = \frac{RC}{\rho}\beta + \sqrt{a^2 + b^2} \qquad (1)$$

Where τ is the time constant, RC is the resistance-capacitance pair, β is the succession rate, a and b are current transience and ρ is the current density. The current desnity is also helpful in finding the cross-section for patients with multiple cardiac diseases.

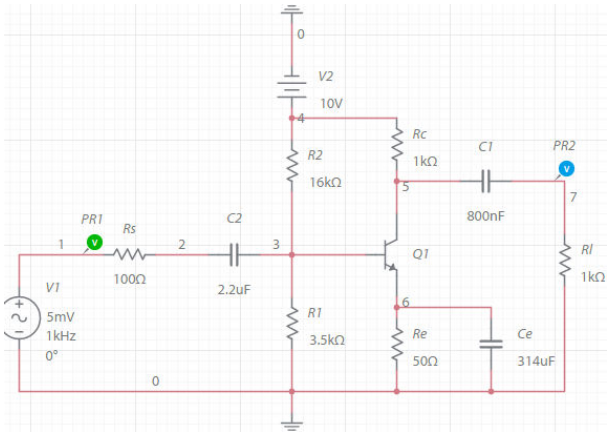

Fig.5. Hemodynamic Lumped Model

Figure 6 shows the output of the hemodynamic model. The transistor helps in the amplification of the flow rate in the case of infraction diseases. The blue and green graphs show the above peak and below peak (before and after the effect) respectively. The intersection value of 6.549 mV is the flow potential and 445.60 microseconds is the time constant for the given data.

| e-ISSN: 2278 – 8875, p-ISSN: 2320 – 3765| www.ijareeie.com | Impact Factor: 7.282|

|| Volume 11, Issue 2, February 2022 ||

DOI:10.15662/IJAREEIE.2022.1102015

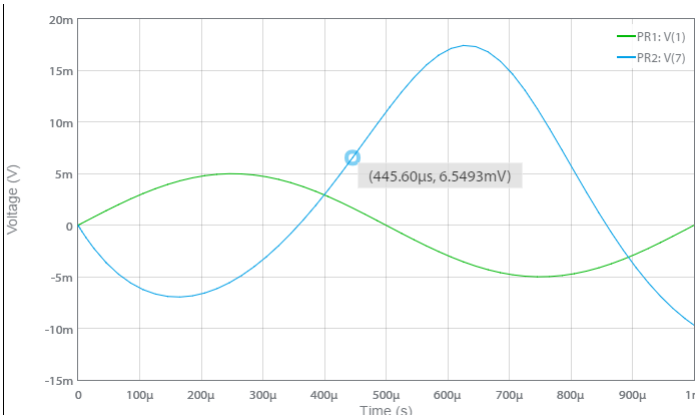

Fig. 6. Hemodynamic Lumped Output

II. LITERATURE REVIEW

- Zhang et al[1]. worked in a pulse pressure-based cardiovascular model where the subjects were from the age group of 50 – 60. The stimuli induced were amplified and step-wise regression was performed to determine age-related medical conditions in the subjects. The nomogram thus obtained was used to develop a one-level model. Input calculations for blood pressure were taken manually using a sphygmomanometer. However, the model was not suitable for multiple parameters and showed skewness in the output. This could sometimes lead to false predictions.
- Grey et al[2]. worked on precision-based static modeling for random trails obtained from predefined data. The data involved heat stimuli injection to patients and their corresponding response. Based on the internal cardio-tolerance (which is the succession response to stimuli marked by an increase or decrease in heart rate for a temporary interval), the response was either increasing exponential or decreasing exponential curve. The point of peak of cure depletion was taken as a model factor. The model fails for dynamic properties and only relies on the stimuli. Non-stimuli conditions were not considered.
- Charles et al[3]. worked on 12 lead ECG electrode configurations to acquire the data from the subjects of age group 40 – 50 before and after load lifting exercise. The data were filtered for QRS complex segmentation which was patterned with myoplasmic concentration (movement of cardiac muscles) to derive the flow model for various periods. The kinematics was constructed using maxwell's models and the differential solutions were derived. The model describes the dynamic properties but is limited to linear responses. Non-linear responses are hard to interpret due to the loss of information in the model.
- Liu et al[4]. worked on a systemic vessel model where Stroke volume along with RR interval for every ECG pulse was calculated. The computational model was simulated in cardiosim for a reduced heart beat. The baroreflex model for open-loop and closed-loop systems was verified. Effector muscle action was taken as the control unit. The system was cross verified with Photoplethysmography (blood volume changes due to illumination input) and a correlation was plotted. The model fails for instantaneous application as the stimuli can only be applied in discrete units. The model does not rely on a threshold and can lead to different results for different age groups due to interior cardio-tolerance levels.
- Spilker [5] derived the mechanical model by considering the interaction between one diastolic period and the elastic artery branch as one unit. Similar branch flow was taken for different time instances and a pressure graph was plotted. The total peripheral resistance and central capacitance were modeled to calculate the flow viscosity in a single circulation. A new parameter – stress on the valves was also taken into account which increased the accuracy of the model. The model limits the application only to manual data input and fails to take successive inputs from the output block (garage values).
- Anderson et al[6]. worked on state equations for tracheal bidirectional airflow by considering the state loop features of the bronchioles. The combination of partial transmural and alveolar pressure described the contraction of the diaphragm during inspiration. The model was also described for the respiratory muscle pressure followed by volume loss in the exchange of air. However, when the model is combined with hemodynamics, the linearity is lost as the model ends up in a transient state[17].

| e-ISSN: 2278 – 8875, p-ISSN: 2320 – 3765| www.ijareeie.com | Impact Factor: 7.282|

|| Volume 11, Issue 2, February 2022 ||

DOI:10.15662/IJAREEIE.2022.1102015

To sum up, some of the limitations of the current models are:

- Instant calibration is possible.
- The model can check the features either in static or dynamic conditions and not both.
- Not suitable for all age groups as it depends on the cardio–tolerance level.
- Skewness exists and exact physiology cannot be mimicked.
- Continuous monitoring is not possible due to discrete levels.

III. SYSTEM ARCHITECTURE

Figure 7 shows the system architecture (work flow) of the proposed model. A detailed explanation of each block is given below.

A. Data Collection

As the model is completely simulation-based, the data is collected from an open-source platform like Physiopedia. The data contains two sets of signals overlapped with each other – spirogram (signal communication in the lung tissues) and electrocardiogram (cardiac rhythm signals). A suitable modulation technique has to be applied to clean the data to remove artifacts like line interference, overshoot and undershoot noises, and non–periodic rhythms. Carrier frequency shaping can be applied to separate the signals without affecting their features. The signals are taken from a subject with a condition of arrhythmia and COPD[9]. At the time of data acquisition, the patient will be exposed to a stimulus for 10 – 20 seconds like heat or illumination to excite the cells. Bolus injection can also be done if the subject experiences gut-related issues.

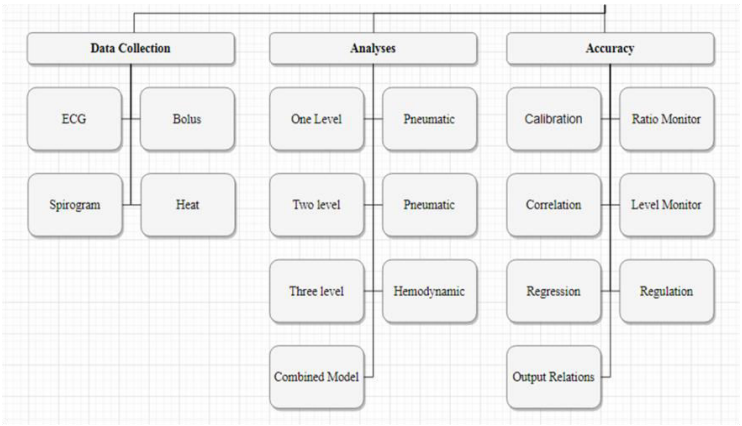

Fig.7. System Architecture

B. Analyses

Suitable Voight models will be constructed for one level to four-level dynamic and the model will be observed for static and dynamic features of the blood flow. To overcome the limitations of the existing models, different parameters like signal origin and dynamic overshoot will be considered. The accuracy and exactness for all the levels will be cross verified by introducing the model to both healthy and abnormal signals. Separate pneumatic and hemo models will be constructed which will be interfaced at the end to provide the ultimate requirements and ratios. The model can also be extended to multiple levels based on the training period and acquired succession rate.

C. Accuracy

Unsupervised regression followed by auto and cross-correlation will be performed to depict and decode the signal features at different temperature and blood pressure conditions. As the breath rate increases during exercise, different scenarios will be incorporated into the model to train and test the Simulink model. Valve level monitors and output: input relations will be determined based on the correlation results.

IV. DATA CLEANING AND PROCESSING

The data collected from the CPR PUCK software for five subjects will be primarily cleaned by removing the above threshold values. Amplitude modulation is then performed to separate the two signals. The ECG wave is taken as the

| e-ISSN: 2278 – 8875, p-ISSN: 2320 – 3765| www.ijareeie.com | Impact Factor: 7.282|

|| Volume 11, Issue 2, February 2022 ||

DOI:10.15662/IJAREEIE.2022.1102015

carrier signal as the number of samples considered is more. The spirogram is the message signal. The Simulink modulation block is shown in figure 8.

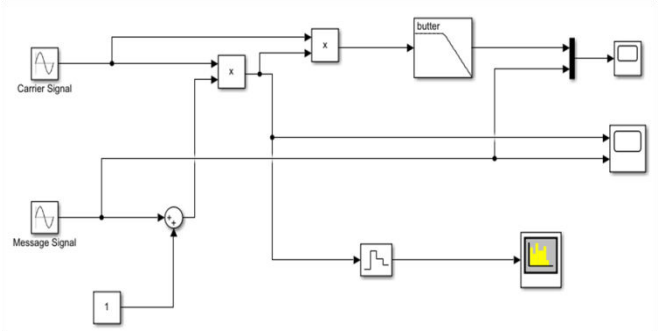

Fig.8. Amplitude Modulation

Only the sinusoidal components of the waves are considered to determine the spectral properties. The buffer filter used is the FIR low pass Butterworth filter with an edge frequency of 8 rad/sec (this frequency is based on the highest spectral peak in the dataset). The order or the filter is set to 8 taps to neutralize the impulse function effect of the signal. Figure 9 shows the overlapped signal before modulation.

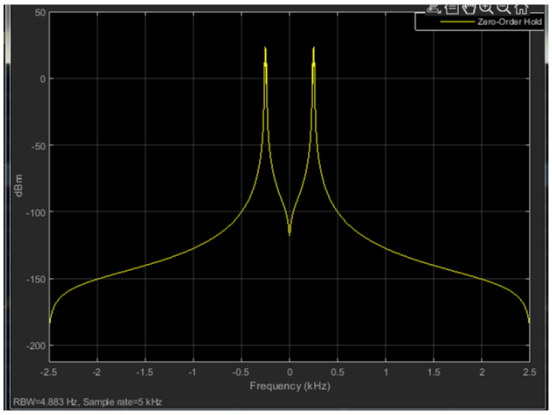

Fig.9 Unmodulated Signal

The modulation is done for a zero ordered equation as the parameter considered is only the amplitude. Figure 10 shows the modulated output with carrier and message signal. It is observed that the overshoot peak to peak is higher for ECG compared to SPG for one breath. Since buffer filters are used, no phase delay is seen in the signals. This improves the accuracy of the study.

Figure 10 the variation in the peaks of the signal when the sampling rate and carrier frequency are changed. This shows the analog properties (continuous) of the signal thus definition it for every interval (deterministic model).

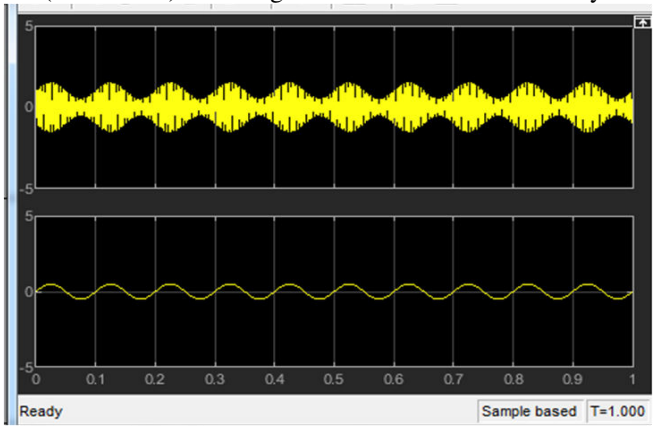

Fig.10 Frequency-Dependent Resultant Signals

| e-ISSN: 2278 – 8875, p-ISSN: 2320 – 3765| www.ijareeie.com | Impact Factor: 7.282|

|| Volume 11, Issue 2, February 2022 ||

DOI:10.15662/IJAREEIE.2022.1102015

When the input characteristics of the wave are changed i.e ECG as message signal and SPG as a carrier signal, the resultant wave is shown in figure 11. This is not an ideal feature as phase and peak delays arise after the steady-state period.

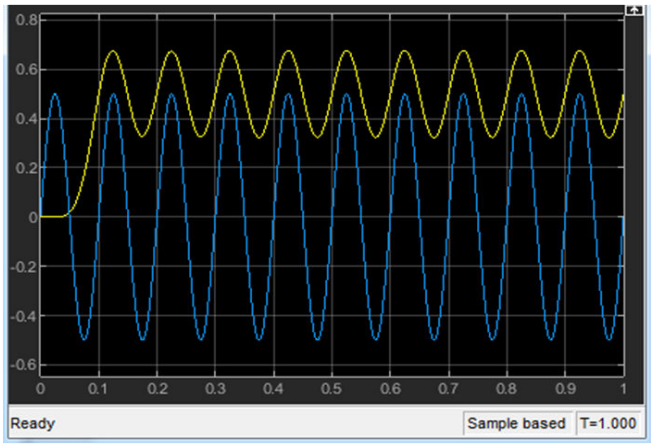

Fig.11. Non – Ideal Wave Nature after T=1s

V. COMPARATIVE ANALYSES

The main objective of the proposed model is to develop a multipara hemopneumato model that works even for irregular rhythmic and non-linear signals. The base of the model is chosen by comparing deterministic and non-deterministic circuits.

A. Schering's Base

Schering's base has four faces with a parallel RC circuit and a series RC circuit on the opposite faces. The other opposite faces are either a single capacitor or inductor to measure the balancing condition. The inherent inductance is compensated once the filter reaches the steady-state condition. Equation 1 represents the unknown balancing conditions[10].

$$\frac{dR}{dt} = \frac{R1.R2}{C2} \; and \; L = R1.R4.C3 \qquad (1)$$

The above equation holds true only for positive resistance coefficient sensors like voltage sensors. Figure 12 shows the model. The rectification is carried out by the diodes of each two in forwarding bias during one positive cycle.

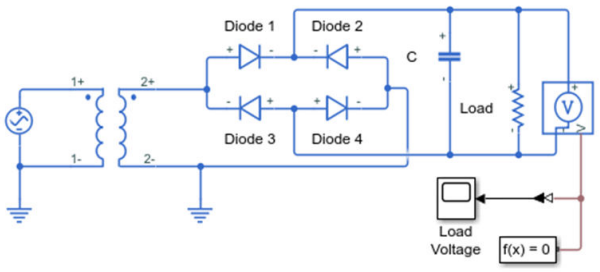

Fig.12. Schering's Model

Figure 13 shows the corresponding zero crossing and sensor output. The pulse width of every two alternate samples has remained constant implying that variability is accepted by the model. The zero crossings are initialized only from 0.005T and not from the origin making it ideal for continuous type signals.

| e-ISSN: 2278 – 8875, p-ISSN: 2320 – 3765| www.ijareeie.com | Impact Factor: 7.282|

|| Volume 11, Issue 2, February 2022 ||

DOI:10.15662/IJAREEIE.2022.1102015

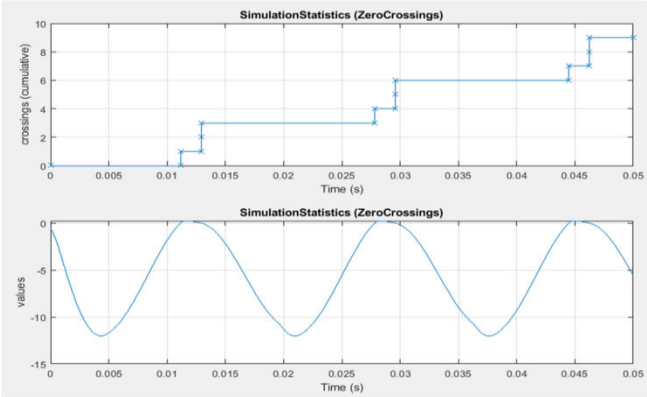

Fig.13. Schering's Model Output

B. Kelvin Voight Base

This model constitutes three blocks – spring (variable passive component), mass (loading component which is blood and pressure in our case), and a damper (tuner which is valve parameter in our case). Equation 2 represents constitutive the relation between the above three factors[11].

$$\sigma = -pI + c1d + c2d2 \qquad (2)$$

Where p is an arbitrary/partial hydrostatic pressure and c1 and c2 are functions of the non-zero invariants of d, d is the diameter of the cell valve. The summation implies the total hydrostatic constituvity. As the function rate increases, the pressure upregulates showing moderate peak breaks in the original wave. Figure 14 shows the base model. The mass and spring system act parallel to each other thus dividing the current (blood) between various branches (arterioles and veins). The stiffness and damping parameter depends on the age of the patient (as per the dataset taken). The transfer function 1/s corresponds to the step input which acts as the error signal monitoring module. Signals beyond the origin point boundary are eliminated by the step module to ensure positive damping.

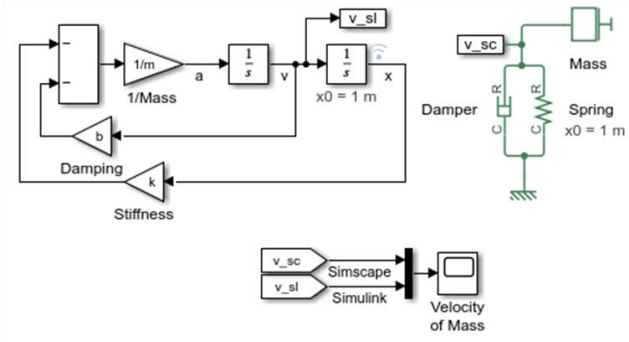

Fig.14. Kelvin Voigt Base Model

The gain of the entire control system is determined by the forward path gain which is in this case $1/ms^2$. The loop gain is bk and the total transfer function determines the stability of the system. Figure 15 shows the stability criterion and the output of the model. We see that the response obtained is underdamped with mid-peak variability. Hence it is an ideal base with strict stability.

| e-ISSN: 2278 – 8875, p-ISSN: 2320 – 3765| www.ijareeie.com | Impact Factor: 7.282|

|| Volume 11, Issue 2, February 2022 ||

DOI:10.15662/IJAREEIE.2022.1102015

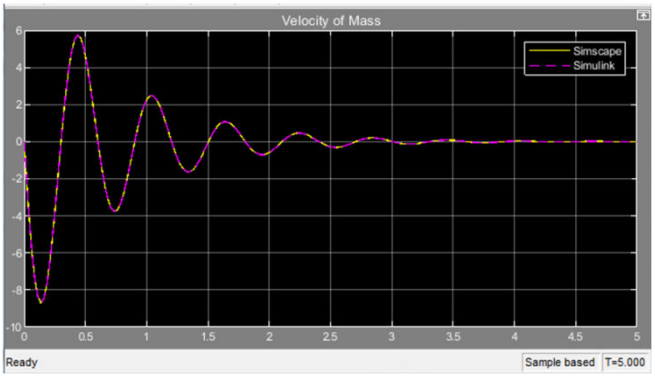

Fig.15. Kelvin Voight Base Output

The other stability criterion is the power dissipated. As the response obtained is underdamped, the power dissipated and absorbed must be inversely proportional to each other thus having a low peak variability. Figure 16 shows the power dissipation from time t=0 to sampling time t=t_s.

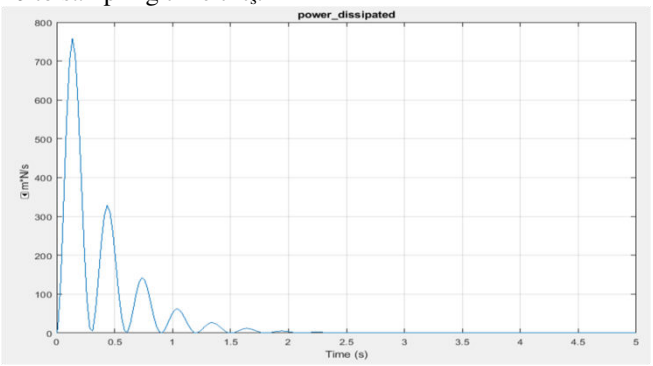

Fig.16. Power Dissipation

VI. ONE-LEVEL PROPOSED MODEL

The one-level hemo-pneumatic model works on determining the arterial behavior by characteristic impedance and volume change. The corresponding relation between the flow and the compliance is seen in equation 3[12].

$$Q = C \cdot s \cdot P + P\,Rp = P\,(s \cdot C + 1\,Rp) \quad (3)$$

Where Q is the flow, c is the compliance represented by capacitor charge and discharge, s is the transfer coefficient, P is the pressure represented by the base module. Rp is the upper airway pressure. By taking Laplace transforms on both sides of equation 3, we get the final relation between blood flow, compliance, and airway pressure variations as seen in equation 4[14].

$$\Delta Q = C\frac{dP}{dt} \quad (4)$$

Where Q is the flow rate, C is the compliance and P is the pressure. It is observed that the change in the rate of flow is directly proportional to the change in pressure. Figure 17 shows the proposed one-level model corresponding to the relation derived.

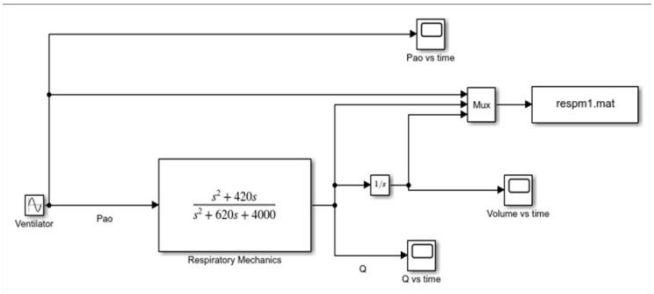

Fig.17. One - Level HemoPneumato Model

| e-ISSN: 2278 – 8875, p-ISSN: 2320 – 3765| www.ijareeie.com | Impact Factor: 7.282|

|| Volume 11, Issue 2, February 2022 ||

DOI:10.15662/IJAREEIE.2022.1102015

The input is the sinusoidal characteristic of the chosen dataset followed by the pulmonary control mechanism. The output values are stored in the MATLAB workbench. Figure 18 shows the pressure versus time and volume versus time relations concerning flow and compliance. We see that the peak Vpp achieved for the message signal is higher than that of the carrier signal.

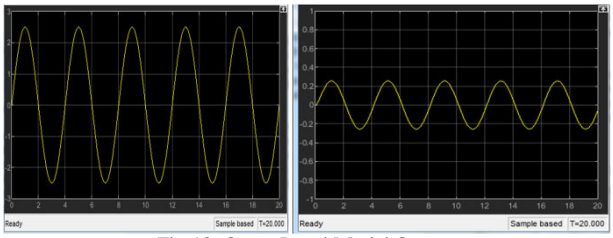

Fig.18. One – Level Model Output

Table 1 shows the output results with their statistical frequency levels for seven trials.

TABLE I. MODEL RESULTS

Parameter	Properties		
	Units of Freedom	*Frequency (Hz)*	*Vpp (V)*
P vs t	5	2.5	20
V vs t	3	23	30
Pao vs t	4	8.3	25
C vs t	-	2	14

VII. TWO–LEVEL PROPOSED MODEL

This is similar to one level model except two more parameters are added - valve cross-section and phase cross-over frequency. The significance is as follows.

- Abnormal restriction to the blood flow is determined by the cross-sectional area.
- Valve impedance is reduced due to the effect of blockage of any fluid which is thus related to its viscosity.

The consecutive equation of the proposed model is seen in equation 5[15][16].

$$P(i) = 1\,Rp + \Delta t\,C \cdot [Q(i) \cdot (Rp \cdot \Delta t)\,C + P(i-1) \cdot Rp] \quad (5)$$

Where P(i) is the pressure varied with the iteration time constant, C is the compliance and R is the resistance across the base spring. Artifacts in the circuit can be constantly monitored by adding a complementary cable resistance. Figure 18 shows the two-level proposed model. An additional gain of 0.5 is added to stabilize the system. During overdamping situations, the gain can be activated to shift the poles to the origin. Figure 19 shows the two-level monitoring system.

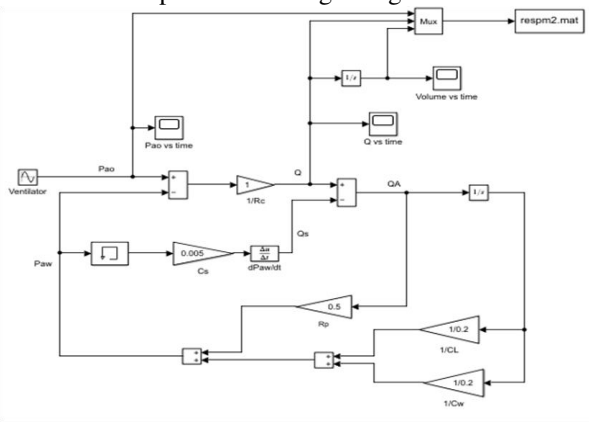

Fig.19. Two – Level Model

Each of the loop gains is iterated back to the input to reach the steady-state point earlier which is an advantage of the proposed model. This makes the model auto calibrated. Each time the dataset is changed, the module gets updated in

| e-ISSN: 2278 – 8875, p-ISSN: 2320 – 3765| www.ijareeie.com | Impact Factor: 7.282|

|| Volume 11, Issue 2, February 2022 ||

DOI:10.15662/IJAREEIE.2022.1102015

the summation block thus alarming the circuit if the parameters vary from the known threshold values. Table 2 tabulates the response of the model as pushed to the MATLAB workbench for seven trials. We see that the Vpp for two level model is higher than the one-level model thus making it more accurate and reliable.

TABLE II. MODEL RESULTS

Parameter	Properties		
	Units of Freedom	*Frequency (Hz)*	*Vpp (V)*
P vs t	3	10	25
V vs t	2	12.03	40
Pao vs t	3	8.5	30
C vs t	-	5.67	10.5
Q vs t	0	25	25

VIII. HYDRAULIC SYSTEM (HEMO – MODEL)

Figure 20 shows the proposed hemodynamic model and its sub - blocks are explained in detail below.

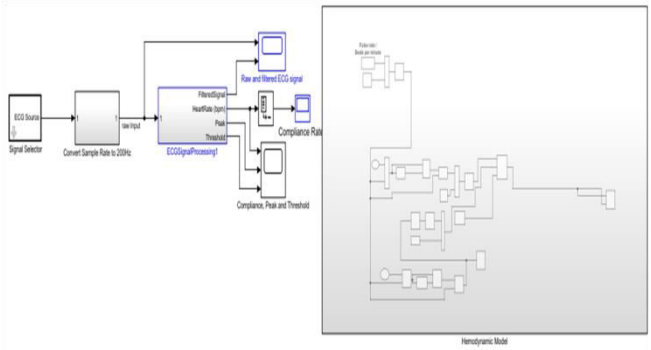

Fig.20. Hydraulic System

A. *ECG Signal Selector*

Since our target focus is blood flow around the circulatory valves, we segment out the QRS complex from the entire ECG sample by designing a hamming FIR windowed filter with a sampling rate 10 times that of the ECG frequency with fixed allocated quantization and direct cascading. Figure 21 shows the FIR block with its windowing equation see in equation 6[13].

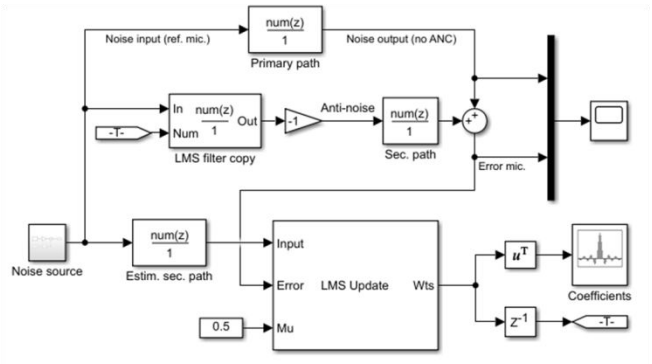

Fig.21. QRS FIR Filter

$$y(n) = b(1)\,x(n) + \cdots + b(n)\,x(1) - a(2)\,y(n-1) - \cdots - a(n)\,y(1) \qquad (6)$$

Where b1 to bn are cosine coefficients and a1 to an are sine coefficients of the window. Figure 22 shows the filter response and the corresponding filtered signal (QRS segment of the input dataset which is fed as the input to the main

| e-ISSN: 2278 – 8875, p-ISSN: 2320 – 3765| www.ijareeie.com | Impact Factor: 7.282|

|| Volume 11, Issue 2, February 2022 ||

DOI:10.15662/IJAREEIE.2022.1102015

model). The signal oscillates between –Vpp to +Vpp thus lying within the threshold values. There are two iterations provided in the filter – Forward and reverse to promote impulse and ramp response respectively. The filter coefficients are updated depending on the iteration the user chooses. The Mu coefficient is the gain adaptive control of the filter. The blue line indicates the artifact error which drastically reaches the negligible value. Sometimes, due to massive data storage, the model is susceptible to errors which can be reduced by self-assessing tools.

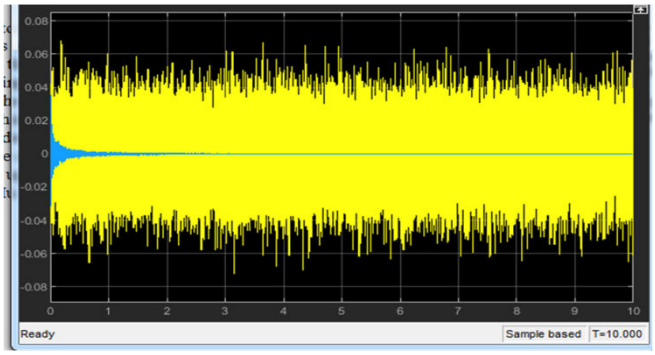

Fig.22 Filtered Output

For every positive and negative peaks, the filter coeffiecients are updated from 1 to 0 and vice versa.

B. Sample Rate Converter

This block has three compounds – input probe (to connect the subsystems), buffer (a component of FIR low pass filter with sampled frequency), and sample rate converter to satisfy the Nyquist law.

C. Processing Unit

This block contains a differentiator to convert impulse responses to unit step responses, a QRS complex detection block, and an FIR bandpass filter to allow –Fs to +Fs frequency signals. The corresponding peak and cyclic average values are calculated. Figure 23 shows the output response of the model and the results are tabulated in Table 3.

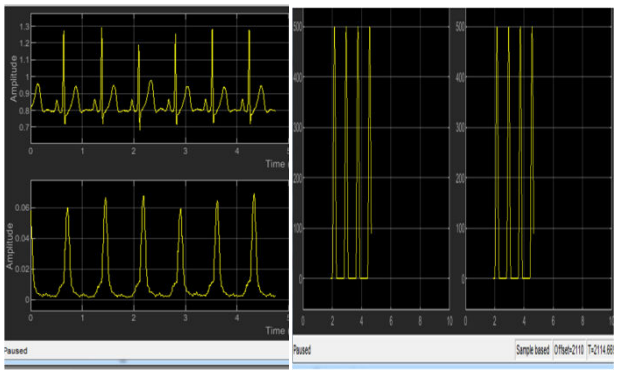

Fig.22. Model Response

The figure on the left is the input and the processed ECG and the figure on the right is the peak response after steady state.

IX. ANALOG MODEL (PNEUMATIC)

Figure 23 shows the proposed pneumatic model. The subsystem contains the pressure, elastance, and volume pressure in parallel combinations which signify the following.

- Elastance: the complex shape memory property of the lungs
- Valve – heater combination: arterial and alveolar air exchange
- Ventilator: external supportive mechanism (mass damper pair)
- Sensors: MATLAB Coded voltage and current sensor to check valve compatibility

| e-ISSN: 2278 – 8875, p-ISSN: 2320 – 3765| www.ijareeie.com | Impact Factor: 7.282|

|| Volume 11, Issue 2, February 2022 ||

DOI:10.15662/IJAREEIE.2022.1102015

The 'check valve' function monitors for negative or positive pressure values (valve open and closing function). The other parameters monitored along with their corresponding functions are:

- Valve and intermediate temperature are given by the function f(x)=ct where c is the transfer coefficient.
- Stuck at 1 or 0 error. Sometimes, due to massive data storage and usage, the activation functions fail to update the weights which might result in overlapping of signal data which leads the pulse train to stay high or low all the time. Irrespective of changes in the input, the output remains the same decreasing the accuracy. This error can be mitigated by using a control signal function which is either a ramp or parabolic signal. The input signal will br overfitted on the control signal to detect the error. If the peak points matches, the control signal data will be compensated with the signal data.
- There are two forward pathways – one is if the input ventilator pressure is higher than the assumed pressure and the other is when the input ventilator pressure is less than the assumed pressure. In the former case, the forward path one is chosen and in the latter case, the forward path two is chosen. The system can be extended with a user button option to set and choose the paths based on the application.

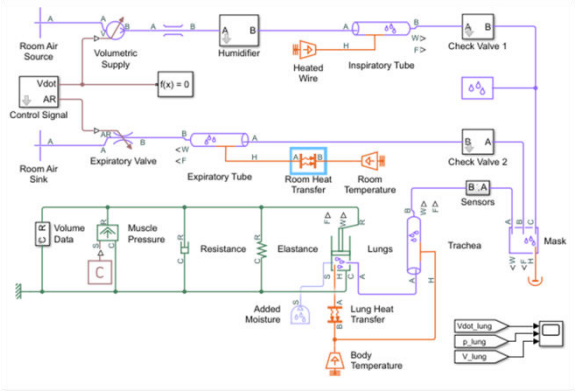

Fig.23 Analog Model

Figure 24 shows the output of the pneumatic model. There are three curves – pressure, volume, and flow versus time. We see that the capacitor discharge time (lung contraction time) is more compared to the capacitor charge time (lung relaxation time). The peak value shifts from positive to negative for every peak value.

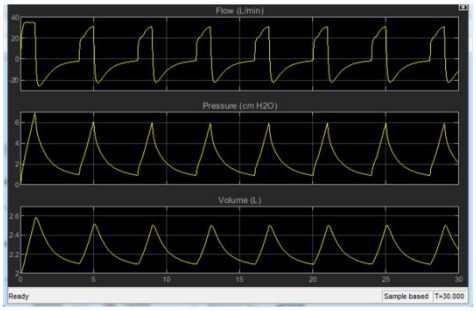

Fig.24. Analog Model Output

X. ACCURACY CHECKER

The output wave and its characteristics were verified using Maxwell's base in multisim. Figure 25 shows the model constructed using multisim. It has three parts:

- Amplification: A non-inverting amplifier is used with piece-wise data having a CMRR of 300 with a gain of 500. This gain can be varied by using a computed resistor across the inverting channel.
- FIR Filter: A FIR bandstop filter is constructed to remove the 50 Hz interference noise in the circuit due to capacitor charge and discharge.
- First-order filter: A first order high pass filter is constructed to allow only the piecewise frequency signals to get amplified.

| e-ISSN: 2278 – 8875, p-ISSN: 2320 – 3765| www.ijareeie.com | Impact Factor: 7.282|

|| Volume 11, Issue 2, February 2022 ||

DOI:10.15662/IJAREEIE.2022.1102015

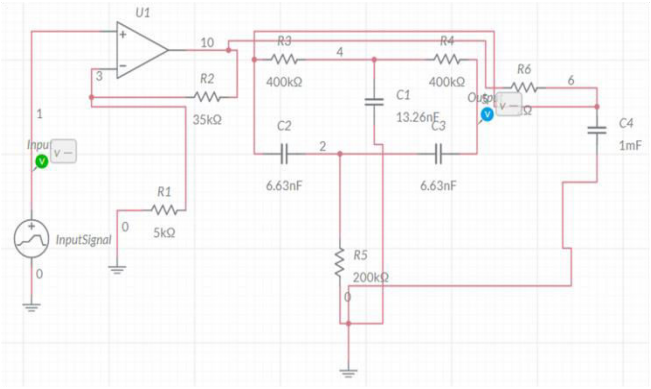

Fig.25. Accuracy Checker

Figure 26 shows the corresponding output. The blue probe is the lung model output (compliance Vs time) and the green probe is the hemo model output (ECG Vs time). We see that the waves' peaks are matching with the previously obtained results with approximate diagonal signal intersection points. This shows that the proposed model is accurate to be used in hospitals. We see that after a certain time, both the outputs overall with each other. This point is called the time of dead zone. This is an important parameter for the clinician to understand the patient's lungs and heart.

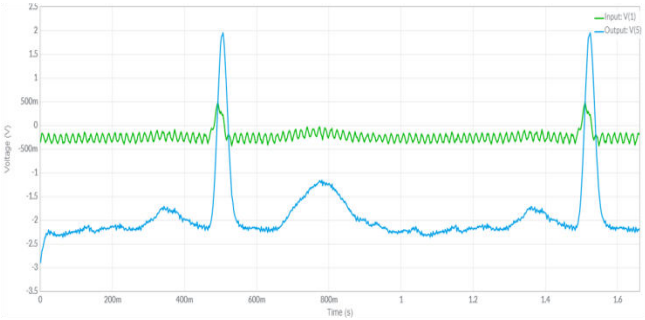

Fig.26. Accurate Model Output

XI. Discussion and Future Scope

Thus hybrid real-time data was acquired to feed it into the four-level pneumatic and hemo models and the following conclusions were obtained.

- An increase in taps of the FIR windows led to loss of information in the signals (eg: the backend signal peaks were not volleyed). This is mainly due to the suppression property of the FIR filter. Hence the FIR's taps should be maintained less than or equal to 25 for optimum performance.
- To expose the circuit to the testing phase, a valve subsystem was developed and was interfaced with the model as seen in figure 27. This will subject the model to additional pressure and flow differences and determine the error and static sensitivity. A delay is introduced where the pressure to the area (plasticance property) is the back propagated loop gain.

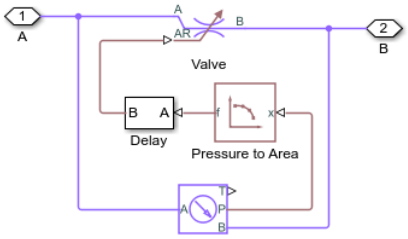

Fig.27. Valve Subsystem

| e-ISSN: 2278 – 8875, p-ISSN: 2320 – 3765| www.ijareeie.com | Impact Factor: 7.282|

|| Volume 11, Issue 2, February 2022 ||

DOI:10.15662/IJAREEIE.2022.1102015

- The compliance and the volumetric flow rate can be determined by the control signal subsystem as seen in figure 28. A forward gain of one can help in preventing impulse level unstableness so that the entire system maintains marginal stability.

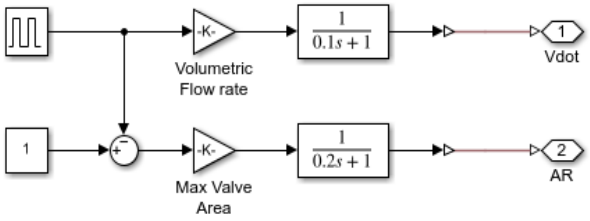

Fig.28. Control Subsystem

Table 3 summarises the results obtained.

TABLE III. RESULTS OBTAINED

Parameter	Properties		
	Units of Freedom	*Frequency (Hz)*	*Vpp (V)*
Complaince	3	10	25
Flow rate	2	12.03	40
Dynamic ratio	3	8.5	30
Sampling error	-	5.67	10.5
Q vs t	0	25	25

The future scope of the project is to fabricate the same into a product by reducing the redundancy error and increasing the correlation ration between the carrier and the message signal. The hardware has to be interfaced with the HEXOSYS frame (medical device software) to understand and interpret the spirogram and ECG.

- Spirogram: The wave has two crests and a trough. The plateau region is the underpotential region with zero tolerance level which is linear for COPD patients.
- ECG: The peak region following ventricular repolarization is of a significant role in determining ailments.

XII. CONCLUSION

Since the current era is biosignals, it can play a huge role in diagnosis and therapy. Current technologies are limited to etracing only encephalogram and cardiogram. The proposed model tends to measure the hemo and pneumatic parameters like the spirogram and cardiohemogram. The algorithm first measures a suitable model base considering multiple differential abilities followed by comparing one-level and two-level hemo models for accuracy. The entire thoracic physiological model was developed into a mechanical model in Simulink and was verified for feasibility and accuracy using Multisim. The model was able to continuously monitor the compliance rate and output the required graphs. Datasets for healthy and abnormal conditions were chosen which were denoised to get the targeted signals. The model can be extended into a stand-alone device for usage in tiered hospitals.

REFERENCES

[1] X. Zhang, D. Wu, F. Miao, H. Liu and Y. Li, "Personalized Hemodynamic Modeling of the Human Cardiovascular System: A Reduced-Order Computing Model," in IEEE Transactions on Biomedical Engineering, vol. 67, no. 10, pp. 2754-2764, Oct. 2020, doi: 10.1109/TBME.2020.2970244.

[2] R. A. Gray and P. Pathmanathan, "Patient-specific cardiovascular computational modeling: Diversity of personalization and challenges", J. Cardiovasc. Trans. Res., vol. 11, no. 2, pp. 80-88, 2018.

[3] A. T. Charles, A. F. Timothy and K. M. James, "Computational fluid dynamics applied to cardiac computed tomography for noninvasive quantification of fractional flow reserve", J. Am. Coll. Cardiol., vol. 61, no. 22, pp. 2233-2241, 2013..

[4] H. Liu et al., "Multi-scale modeling of hemodynamics in the cardiovascular system", Acta Mech. Sin., vol. 31, no. 4, pp. 446-464, 2015.

[5] R. L. Spilker et al., "Morphometry-based impedance boundary conditions for patient-specific modeling of blood flow in pulmonary arteries", Ann. Biomed. Eng., vol. 35, no. 4, pp. 546-559, 2007.

| e-ISSN: 2278 – 8875, p-ISSN: 2320 – 3765| www.ijareeie.com | Impact Factor: 7.282|

|| Volume 11, Issue 2, February 2022 ||

DOI:10.15662/IJAREEIE.2022.1102015

[6] Anderson RL, Carr JH, Bond WW, Favero MS. Susceptibility of vancomycin-resistant enterococci to environmental disinfectants. Infect Control Hosp Epidemiol. 1997 Mar;18(3):195–199.
[7] Walsh SE, Maillard JY, Russell AD. Ortho-phthalaldehyde: a possible alternative to glutaraldehyde for high level disinfection. J Appl Microbiol. 1999 Jun;86(6):1039–1046
[8] V. Manoliu, "Modeling cardiovascular hemodynamics in a model with nonlinear parameters," 2015 E-Health and Bioengineering Conference (EHB), 2015, pp. 1-4, doi: 10.1109/EHB.2015.7391407.
[9] L. T. Gaudio, M. V. Caruso, S. De Rosa, C. Indolfi and G. Fragomeni, "Different Blood Flow Models in Coronary Artery Diseases: Effects on hemodynamic parameters," 2018 40th Annual International Conference of the IEEE Engineering in Medicine and Biology Society (EMBC), 2018, pp. 3185-3188, doi: 10.1109/EMBC.2018.8512917.
[10] L. Wang et al., "Hemodynamic Analysis of Pulmonary Arterial Hypertension Associated with Congenital Heart Disease: A Numerical Study of Patient-Specific Models," 2018 11th International Congress on Image and Signal Processing, BioMedical Engineering and Informatics (CISP-BMEI), 2018, pp. 1-5, doi: 10.1109/CISP-BMEI.2018.8633167.
[11] T. Wang, F. Liang, R. Liu, S. Simakov, X. Zhang and H. Liu, "Model-Based Study on the Hemodynamic Effects of Graduated Compression Stockings in Supine and Standing Positions," 2018 IEEE-EMBS Conference on Biomedical Engineering and Sciences (IECBES), 2018, pp. 27-31, doi: 10.1109/IECBES.2018.8626656.
[12] F. Shang, Z. Li, L. Li and D. Guo, "Modeling of Airflow-Based Lung Sound for Characterization of Bronchi," 2018 12th IEEE International Conference on Anti-counterfeiting, Security, and Identification (ASID), 2018, pp. 245-249, doi: 10.1109/ICASID.2018.8693117.
[13] T. Shimoda, Y. Obase, Y. Nagasaka, H. Nakano, R. Kishikawa and T. Iwanaga, "Lung sound analysis and airway inflammation in bronchial asthma", Journal of Allergy & Clinical Immunology in Practice, vol. 4, no. 3, pp. 505-511, 2016.
[14] O. H. Wittekindt, "Tight junctions in pulmonary epithelia during lung inflammation", Pflugers Archiv, vol. 469, no. 1, pp. 135-147, 2017.
[15] M. Y. Chen and C. H. Chou, Applying Cybernetic Technology to Diagnose Human Pulmonary Sounds, Plenum Press, 2014.
[16] S. Abbasi, R. Derakhshanfar, A. Abbasi and Y. Sarbaz, Classification of normal and abnormal lung sounds using neural network and support vector machines, 2013.
[17] R. Palaniappan, K. Sundaraj, N. U. Ahamed, A. Arjunan and S. Sundaraj, "Computer-based respiratory sound analysis: A systematic review", Iete Technical Review, vol. 30, no. 3, pp. 248-256, 2013.

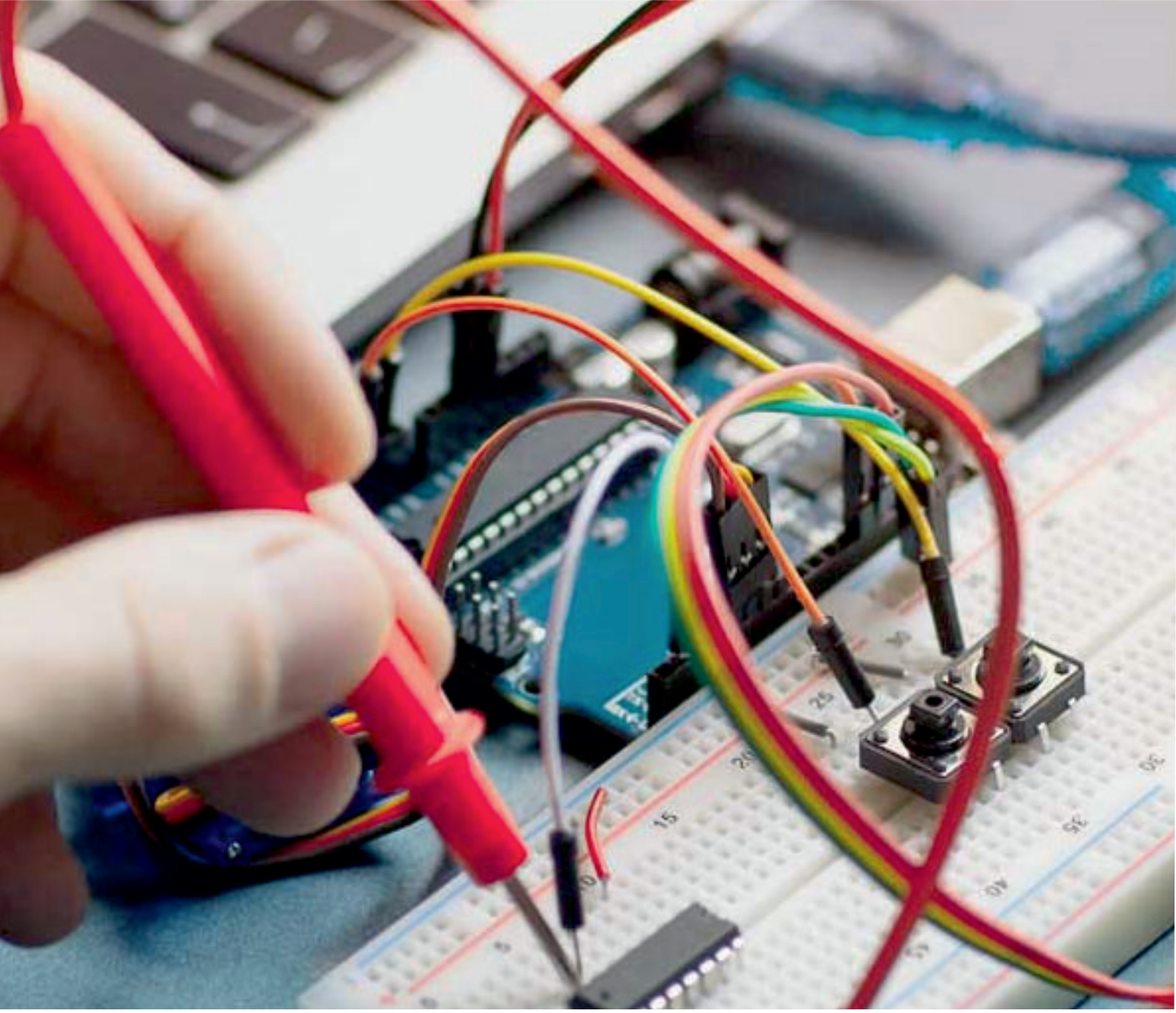

INNO SPACE
SJIF Scientific Journal Impact Factor

Impact Factor: 7.282

doi cross ref

ISSN INTERNATIONAL STANDARD SERIAL NUMBER INDIA

निस्केयर NISCAIR

International Journal of Advanced Research

in Electrical, Electronics and Instrumentation Engineering

9940 572 462 6381 907 438 ijareeie@gmail.com

www.ijareeie.com

Scan to save the contact details